

Verification of the Numerical Simulation of Permafrost Using COMSOL Multiphysics® Software

E. E. Dagher¹, G. Su¹, and T.S. Nguyen¹

¹Canadian Nuclear Safety Commission, Ottawa, ON, Canada

Abstract: Different modelling tools, including COMSOL Multiphysics® (COMSOL) finite element method (FEM) simulation software can be used in understanding complex thermal and hydrogeological effects. COMSOL was used to simulate the conductive heat transfer with phase change in the geological formations encompassed in permafrost surrounding a shallow thaw lake. The purpose of the simulation was to verify the adequacy of COMSOL to model such phenomena by comparing the COMSOL results to those obtained by another FEM model (Ling and Zhang, 2003). The graphical comparison of the simulation results show that they are in agreement with those published by Ling and Zhang (2003).

In light of the obtained results, COMSOL can be used to adequately model the time-dependent conductive heat transfer with phase change and assess the thaw effects due to a shallow thaw lake over continuous permafrost. The verification of this study provides evidence that the COMSOL code can be applied to more complex multiphysics problems. This includes the modelling of coupled heat transfer (conduction and convection with phase change) and groundwater flow in order to determine the thaw effects surrounding a uranium in-pit TMF in continuous permafrost.

Keywords: permafrost, heat transfer, phase change, talik formation, numerical modelling

1. Introduction

The thaw potential of warm uranium tailings disposed in an in-pit tailings management facility (TMF) and constructed in continuous permafrost could potentially influence future long-term contaminant migration. An understanding of the coupled processes of heat transfer (conduction and convection) with phase change and groundwater flow is needed to assess the changing thermal regime of a TMF and surrounding geological formations, as well as to determine the potential thaw effects which may lead to permafrost degradation and talik development beneath a TMF. Different modelling

tools, including COMSOL Multiphysics (COMSOL) finite element method (FEM) simulation software, can be used in understanding these complex thermal and hydrogeological effects. However, in order to assess whether COMSOL could adequately model the coupled multiphysics problem in the application to uranium tailings disposal, verification of a simple model in COMSOL was performed. This simple model is based on that of Ling and Zhang (2003) for the numerical simulation of the permafrost thermal regime and talik development under shallow thaw lakes on the Alaskan arctic coastal plain.

A talik is a layer or body of unfrozen ground within the permafrost (Andersland and Ladanyi 2004). They can be “closed” when completely enclosed within frozen ground, or “open” when partially surrounded. Taliks form under thawed water bodies for which the lake or stream does not completely freeze through during the year. These water bodies provide a heat source for the frozen ground underneath, and this temperature gradient drives permafrost degradation and talik formation (Burn 2002; Ling and Zhang 2003; Lawrence et al. 2008).

Over time, the thickness of the talik increases as a function of the waterbody bottom temperature. As taliks form they contribute to further thaw settlement and permafrost degradation, increasing in thickness over time, and potentially causing significant changes to the physical, chemical, biological, and geomorphological processes occurring in the ground (Johnston and Brown 1964). As indicated by Lawrence et al. (2008), taliks form and continue to expand due to accumulation of the soil heat content by the summer heat wave which extends deeper than the winter cooling wave is capable of refreezing during the winter months. This permits heat accumulation with depth as the soil melts.

Extension of a talik to the deep groundwater regime and the formation of an “open talik” may result in significant contaminant migration due to the shifting thermal regime (Biggar 2004). Dyke (2001) reported elevated concentrations of

potassium in the active layer at distances well beyond what would be expected by diffusive transport alone, suggesting that contaminant migration by advection through the soil occurs, because the hydraulic conductivity has increased by up to four orders of magnitude during the freeze-thaw cycle. Tokarev et al. (2006) and Surbeck et al. (2006) observed that high U-234 concentration was found in the water from melting permafrost during permafrost degradation in Russia and Switzerland.

Several studies have been performed to numerically model the talik development under shallow thaw lakes in order to understand the permafrost degradation behavior. These studies have shown significant talik development overtime underneath shallow thaw lakes (Burn 2002; Ling and Zhang 2003).

2. Theory

2.1 Governing Equation

The governing equation used to model the potential for talik development under shallow thaw lakes is the overall transient heat transfer mechanism in porous media, which can be described by the following heat equation:

$$(\rho c_m)_{eq} \frac{\partial T}{\partial t} + \rho_L c_{m,L} \mathbf{u} \cdot \nabla T = \nabla \cdot (k_{eq} \nabla T) + Q \quad [1]$$

where ρ_L is the fluid density in kg m^{-3} , ρ_P is the dry density of the porous media in kg m^{-3} , $c_{m,L}$ is the fluid mass heat capacity at constant pressure in $\text{kJ kg}^{-1} \text{ }^\circ\text{C}^{-1}$, $c_{m,P}$ is the porous matrix mass heat capacity at constant pressure in $\text{kJ kg}^{-1} \text{ }^\circ\text{C}^{-1}$, Θ_P is the volume fraction of the porous matrix, Θ_L is the volume fraction of the fluid, or equivalently the porosity, n , calculated in eq. [2] by,

$$n = \frac{V_v}{V_T} = \theta_L = 1 - \theta_P \quad [2]$$

where V_v is the volume of voids (air and water) in m^3 , V_T is the total volume of the soil in m^3 . $(\rho c_m)_{eq}$ is the equivalent volumetric heat capacity of the solid fluid system in $\text{kJ m}^{-3} \text{ }^\circ\text{C}^{-1}$, and is expressed by eq. [3],

$$(\rho c_m)_{eq} = \theta_P \rho_P c_{m,P} + \theta_L \rho_L c_{m,L} \quad [3]$$

k_{eq} represents the equivalent thermal conductivity in $\text{W m}^{-1} \text{K}^{-1}$ and the conductivity of the fluid, k_L , by eq. [4],

$$k_{eq} = \theta_P k_P + \theta_L k_L \quad [4]$$

\mathbf{u} is the fluid velocity field and should be interpreted as the Darcy velocity, that is, the volume flow rate per unit cross-sectional area in m s^{-1} . The average linear velocity (the velocity within the pores) can be calculated by eq. [5],

$$\mathbf{u}_L = \frac{\mathbf{u}}{\theta_L} \quad [5]$$

Q is the heat source (or sink) in W m^{-2} .

The above overall heat equation for time-dependent heat transfer in porous media takes into account heat transfer contributions from both conduction and convection. The following sections summarize the calculation of material properties required to solve the heat transfer equation.

2.2 Heat Capacity of Frozen and Unfrozen Soils

As stated above in eq. [3], the equivalent volumetric heat capacity of porous media can be computed by adding the heat capacities of the different constituents in a unit mass of the media. For frozen and unfrozen soils the constituents include the solid matrix, water, ice and air. The mass and heat capacity of the soil can then be calculated by eq. [6],

$$c_m = \frac{1}{m} (c_s m_s + c_w m_w + c_i m_i + c_{air} m_{air}) \quad [6]$$

where m_s , m_w , m_i , and m_{air} are the masses of the constituents of the frozen soil, solid matrix, water, ice and air respectively, while c_s , c_w , c_i , and c_{air} are the mass heat capacities of the constituents in the frozen soil, solid matrix, water, ice and air, respectively.

Assuming the contribution due to air is negligible and dividing by the volume, V , the volumetric heat capacity of the soil is therefore defined in eq. [7] as,

$$c_v = c_m \rho_f = \rho_{df} (c_s + c_w w_u + c_i w_f) \quad [7]$$

where ρ_f and ρ_{df} are the bulk and dry densities of the frozen soil respectively, and w_u and w_i are the

unfrozen and frozen water contents respectively. The total water content, w , of a frozen soil is related to the frozen, w_f , and unfrozen, w_u , water content by eq. [8],

$$w = w_u + w_f \quad [8]$$

Using the specific heat of a material defined as the ratio of its heat capacity to that of water, volumetric heat capacity can be calculated in terms of the specific heats of the constituents in the soil. For mineral soils, the specific heats of the solid particles, water, and the ice are 0.17, 1.0, and 0.5, respectively (Andersland and Ladanyi 2004). The frozen, c_{vf} , and unfrozen, c_{vu} , volumetric heat capacities can be calculated by Eq. [9] and [10] respectively,

$$c_{vu} = \left(\frac{\rho_d}{\rho_w}\right) \left(0.17 + 1.0 \frac{w}{100}\right) c_{vw} \quad [9]$$

$$c_{vf} = \left(\frac{\rho_d}{\rho_w}\right) \left[\left(0.17 + 1.0 \frac{w_u}{100}\right) + 0.5 \left(\frac{w-w_u}{100}\right)\right] c_{vw} \quad [10]$$

where ρ_w is the density of water, and c_{vw} is the volumetric heat capacity of water (4.187 MJ m⁻³ °C). It should be noted that the water content in the equation is presented as (% mass). The volumetric heat capacity can be converted back to a mass heat capacity by the expression in eq. [11],

$$c_m = \left(\frac{c_v}{\rho}\right) = \frac{c_v}{\rho_d \left(1 + \frac{w}{100}\right)} \quad [11]$$

To account for phase change, the volumetric latent heat of fusion, L , for the soil can be calculated by eq. [12],

$$L = \rho_d L' \frac{w - w_u}{100} \quad [12]$$

where L' is the mass specific latent heat of fusion for water (at 0°C $L' = 333.7$ kJ kg⁻¹) (Andersland and Ladanyi, 2004). The corresponding volumetric heat capacity during the phase change is therefore,

$$c_v = \begin{cases} c_{vf} & T < T_e - \Delta T \\ c_{pc} = c_{vf} + \frac{\rho_d L' \frac{w - w_u}{100}}{\Delta T} & T_e - \Delta T < T < T_e \\ c_{vu} & T > T_e \end{cases} \quad [13]$$

It should be noted that lowering ΔT , the width of the phase change (or phase change interval) has significant effects on the thermal bulb of the -1°C

isotherm. This is a result of an increase in the importance of the latent heat term which results in increasing the heat capacity during the phase change.

2.3 Thermal Conductivity

Similar to the equivalent heat capacity, the equivalent thermal conductivity of porous media can be computed by adding the thermal conductivities of the different constituents multiplied by their respective volumetric proportions. For soils, many studies have been conducted and methods developed to calculate the thermal conductivity of soils. An extensive review of these methods has been undertaken by Farouki (1981). For natural soils and crushed rock, Kersten (1949) developed empirical equations for frozen and unfrozen thermal conductivities for coarse-grained soils which are predominately quartz (silt-clay content < 20%), expressed in eq^{ns} [14] and [15] respectively,

$$k_u \left(\frac{W}{m \cdot K}\right) = 0.1442(0.7 \log w + 0.4)(10)^{0.6243\rho_d} \quad [14]$$

$$k_f \left(\frac{W}{m \cdot K}\right) = 0.01096(10)^{0.8116\rho_d} + 0.00461(10)^{0.9115\rho_d w} \quad [15]$$

For fine-grained soils (50% or more silty-clay) for which studies weren't performed on, empirical equations developed by interpolation based on quartz content was suggested (Andersland and Ladanyi 2004) as expressed in eq^{ns} [16] and [17],

$$k_u \left(\frac{W}{m \cdot K}\right) = 0.1442(0.9 \log w - 0.2)(10)^{0.6243\rho_d} \quad [16]$$

$$k_f \left(\frac{W}{m \cdot K}\right) = 0.001442(10)^{1.373\rho_d} + 0.01226(10)^{0.4884\rho_d w} \quad [17]$$

These equations are a function of the dry density of the soil, ρ_d in g cm⁻³, and the percent mass water content, w (% mass).

When modelling freeze/thaw conditions phase change must be considered. Lunardini (1981) suggested that the thermal conductivity be calculated by the piecewise function expressed in eq. [18],

$$k = \begin{cases} k_f & T < T_e - \Delta T \\ k_{pc} = k_f + \frac{k_u - k_f}{\Delta T} [T - (T_e - \Delta T)] & T_e - \Delta T < T < T_e \\ k_u & T > T_e \end{cases} \quad [18]$$

It should be noted that lowering ΔT , the width of the phase change (or phase change interval) has significant effects on the thermal bulb of the -1°C isotherm. This is a result of a decrease in the thermal conductivity during the phase change

2.4 Predicting the Frozen Water Content of Unfrozen Soils

The percent water content, w , described on the basis of dry mass of soil can be expressed by eq. [19],

$$w = \frac{M_w}{M_s} (100) \quad [19]$$

Anderson and Tice (1972) showed that below freezing temperature, some water remains in the unfrozen state in frozen soils. Neglecting the vapour phase of soil particles, the total water content can be expressed by eq. [8] above.

The percentage of unfrozen water content in a frozen soil is based on the physical properties of the soil and the soil temperature (Andersland and Ladanyi 2004). As temperature decreases past the freezing temperature, the percent unfrozen water content also decreases. Experimental data by Tice et al. (1976) in which total water contents and various physical properties of several soils were varied, expressed the variation in the unfrozen water content, w_u , as a function of temperature by a simple power curve of the form,

$$w_u = \alpha \theta^\beta \quad [20]$$

where α and β are characteristic soil parameters and θ is temperature, expressed as a positive number in degrees Celsius below freezing. This prediction equation can be used to determine the unfrozen water contents of frozen soils.

3. Use of COMSOL Multiphysics

3.1 Model Description

Ling and Zhang (2003) used a two-dimensional heat transfer model incorporating phase change to investigate the long-term influence of shallow thaw lakes on permafrost thermal regime and talik development. The model was based on the finite element method and was modified from an existing model designed by Ling et al. (2000a; 2000b). The model used a cylindrical coordinate system assuming no

annular heat flow. A schematic illustration of the analysis domain and boundary conditions used for the simulation are presented in Figure 1.

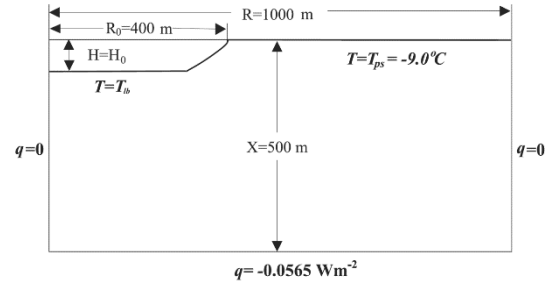


Figure 1. Illustration of analysis domain and boundary conditions for simulation. The upper boundary is set at lake bottom off the shore and at a depth of 0.5 m below the ground surface on the shore (Adapted from Ling and Zhang 2003)

3.2 Model Verification Heat Transfer Physics

Ling and Zhang (2003) used a modified version of the overall heat transfer coefficient and only took into account thermal conduction as the most significant heat transfer pathway. As such the model does not account for the velocity field nor the porosity of the soil matrix, and the effects of thermal convection have been ignored. The modified version of eq. [1] above is expressed in eq^{ns} [21] and [22] for the unfrozen zone and the frozen zone respectively, with the convection term removed and taking into account the cylindrical coordinate system.

Unfrozen zone

$$C_u \frac{\partial T_u}{\partial t} = \frac{\partial}{\partial r} \left(k_u \frac{\partial T_u}{\partial r} \right) + \frac{k_u}{r} \frac{\partial T_u}{\partial r} + \frac{\partial}{\partial x} \left(k_u \frac{\partial T_u}{\partial x} \right) \quad (0 < t < t_{TS}, (x, r) \in \Omega_u) \quad [21]$$

Frozen zone

$$C_f \frac{\partial T_f}{\partial t} = \frac{\partial}{\partial r} \left(k_f \frac{\partial T_f}{\partial r} \right) + \frac{k_f}{r} \frac{\partial T_f}{\partial r} + \frac{\partial}{\partial x} \left(k_f \frac{\partial T_f}{\partial x} \right) \quad (0 < t < t_{TS}, (x, r) \in \Omega_f) \quad [22]$$

These are coupled by the continuous temperature condition, eq. [23], and the conservation of energy condition, eq. [24], at the moving interface between the frozen and unfrozen phases:

$$T_u(S(t), t) = T_f(S(t), t) = T_e \quad (0 < t < t_{TS}) \quad [23]$$

$$k_f \frac{\partial T_f}{\partial n} - k_u \frac{\partial T_u}{\partial n} = L \frac{\partial S(t)}{\partial t} \quad (0 < t < t_{TS}) \quad [24]$$

where $S(t)$ is the phase front position over time, and n is the normal of the phase front position. In COMSOL the Heat Transfer Physics node was selected taking into account conduction only.

3.3 Summary of Soil and Material Properties and Model Parameters

A summary of the soil type of each domain and material properties used by Ling and Zhang (2003) are provided in Table 1, while a list of model parameters used are summarized in Table 2.

Table 1. Physical Properties of Soils Used by Ling and Zhang (2003)

Depth (m)	Soil Type	Dry Density ρ_d , (kg m ⁻³)	Percent Water Content by Mass, w (kg kg ⁻¹)	Unfrozen Water Content by Mass, w_u (kg kg ⁻¹)
0.5-5	Silt	1100	56	4.8
5-50	silt and clay	1200	32	4.8
50-400	gravel and sand	1450	25	3.8
400-500	Gravel	1580	22	3.8

Table 2. Physical Parameters for Verification Model - Simulation Case C4

Parameter	Value	Description
H_0	1.5 m	Lake depth
H_{pal}	0.5 m	Depth of permafrost active layer
R_0	400 m	Lake radius
T_{ps}	-9°C	Mean permafrost surface temperature
T_{lb}	0°C	Lake bottom temperature
T_e	0°C	Permafrost freezing temperature
ΔT	1°C	Width of the phase change interval
q	0.0565 W m ²	Lower boundary constant heat flux
t_{TS}	3000 years	Total simulation time
L_w	333.7 kJ kg ⁻¹	Mass specific latent heat of fusion of water
ρ_w	1000 kg m ⁻³	Density of water
c_{vw}	4.187 MJ m ⁻³ °C	Volumetric heat capacity of water at constant pressure

3.4 Ling and Zhang (2003) Case Studies

Ling and Zhang (2003) conducted their simulations for 11 different cases for which the lake depth and bottom lake temperature were varied as summarized in Table 3. The model verification performed in this study was conducted using simulation case C4 for which results were published. Results of the simulations can be found in Section 4.1.

Table 3. Ling and Zhang (2003) Model Scenarios

Lake Depth, H_0 , (m)	Temperature at Lake Bottom, T_{lb} , (°C)					
	-2.0	-1.0	0.0	1.0	2.0	3.0
1.3	C1	C2	C3			
1.5			C4			
2.0			C5	C6	C7	C8
2.5				C9	C10	C11

3.5 Model Boundary Conditions

A summary of the boundary conditions and initial value condition applied to the model are provided below. As the upper boundary conditions, Ling and Zhang (2003) used Dirichlet boundary conditions where the lake bottom temperature, T_{lb} , and the permafrost surface temperature, T_{ps} , were fixed over the total simulation, $t_{TS} = 3000$ years:

$$T(0.5, r, t) = T_{ps}(t) \quad (0 < t < t_{TS}, x = 0.5, R_0 < r < R)$$

$$T(H_0, r, t) = T_{lb}(t) \quad (0 < t < t_{TS}, x = H_0, 0 < r < R_0)$$

A Neumann boundary condition was applied at the lower boundary with a constant inward heat flux of $q = 0.0565$ W m⁻². This was based on the geothermal heat flux at great depth on the North Slope of Alaska (Lachenbruch et al. 1982; Osterkamp and Gosink 1991).

$$-k \frac{\partial T(X, r, t)}{\partial x} = q \quad (0 < t < t_{TS}, x = X, 0 < r < R)$$

Lateral Boundary Conditions are treated as zero heat flux boundary conditions:

$$\frac{\partial T(x, r, t)}{\partial r} = 0 \quad (0 < t < t_{TS}, H_0 < x < X, r = 0)$$

$$\frac{\partial T(x, r, t)}{\partial r} = 0 \quad (0 < t < t_{TS}, 0.5 < x < X, r = R)$$

3.6 Initial Value Conditions

As the initial value condition for the time-dependent problem, a geothermal gradient was applied across the depth of the model domain. This gradient was approximated by using COMSOL's interpolation function to linearly interpolating (and extrapolating) the temperature between the average annual permafrost surface temperature ($T_{ps} = -9^{\circ}\text{C}$) and the bottom of the permafrost layer (0°C at $x = -400$ m). Figure 2 illustrates the thermal regime through the model at $t = 0$ s, representing the initial condition to the transient solution as simulated in COMSOL.

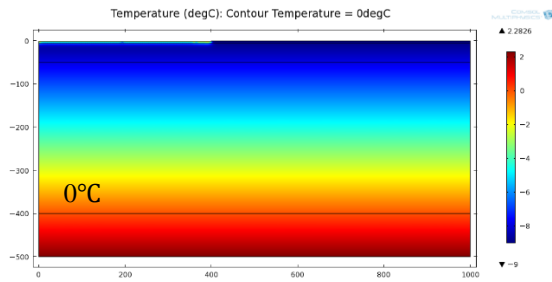


Figure 2. Model at Simulation Time $t = 0$ s

3.7 Geometry and Mesh

The geometry and mesh of the model in COMSOL is presented in Figure 3 below. Due to the simplification of the geometry and co-ordinate system by assuming symmetry at the center of the lake, an extra fine mesh was applied in order to achieve simulation results that were as accurate as could be computationally achieved.

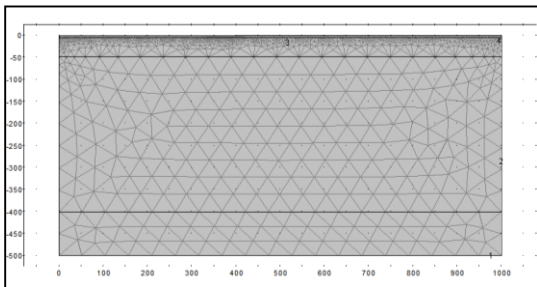


Figure 3. Geometry and Meshing of Model

4. Experimental Results

The results of the model verification in COMSOL are provided below. The verification results in COMSOL are presented in Figure 4 directly compared to those of the simulation case C4 results published by Ling and Zhang (2003). The results are for solution times at 500 years, 1000 years, 2000 years and 3000 years respectively. The images on the left have been adapted from those published by Ling and Zhang (2003). The images on the right are the simulation results from the model verification performed in COMSOL. It should be noted that the images from COMSOL are scaled accurately and the depth is shown from 0 m to 500 m below ground surface, whereas the results of Ling and Zhang (2003) are only presented to the bottom of the permafrost layer. For these reasons the images may look stretched.

Ling and Zhang (2003) did not present results of the steady-state solution. In order to verify the extent of the thaw bulb and degree talik development and permafrost degradation, the model was run under steady-state conditions and the result of the simulation is presented in Figure 5.

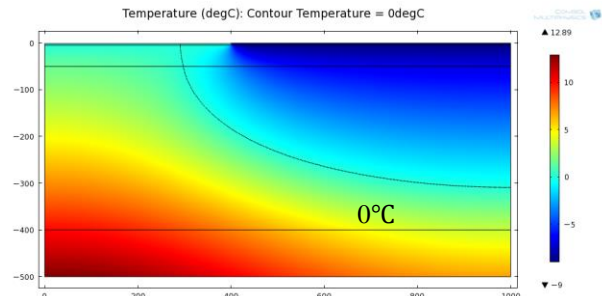
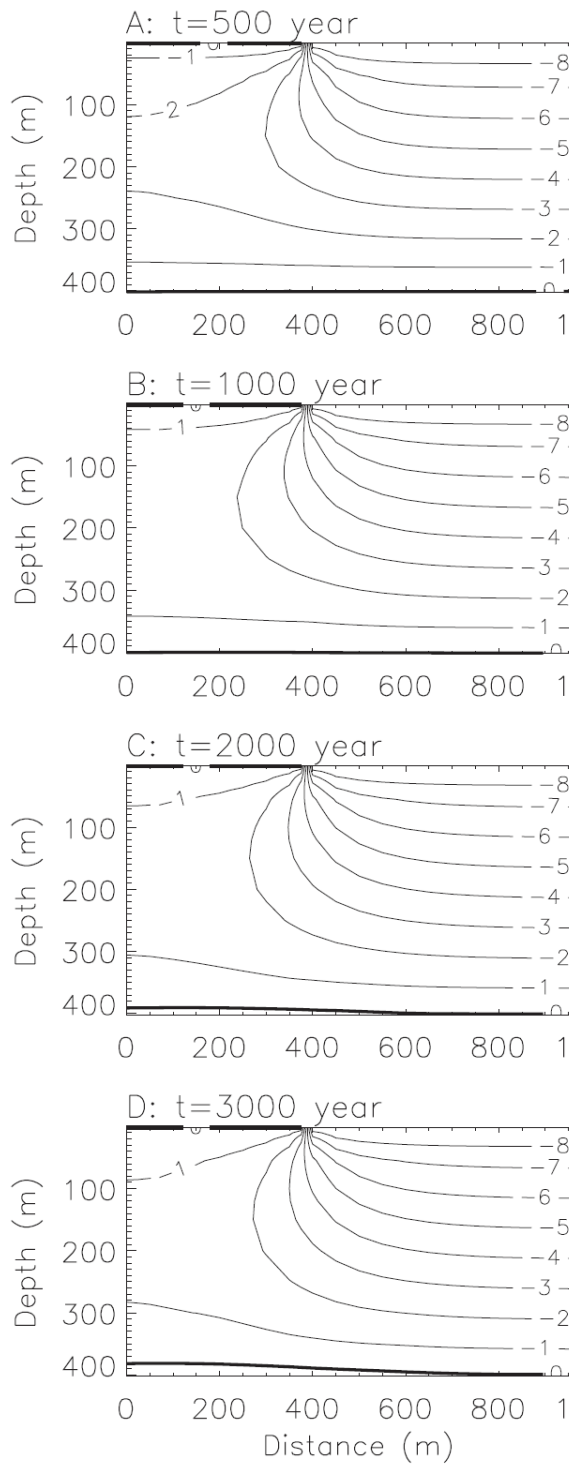
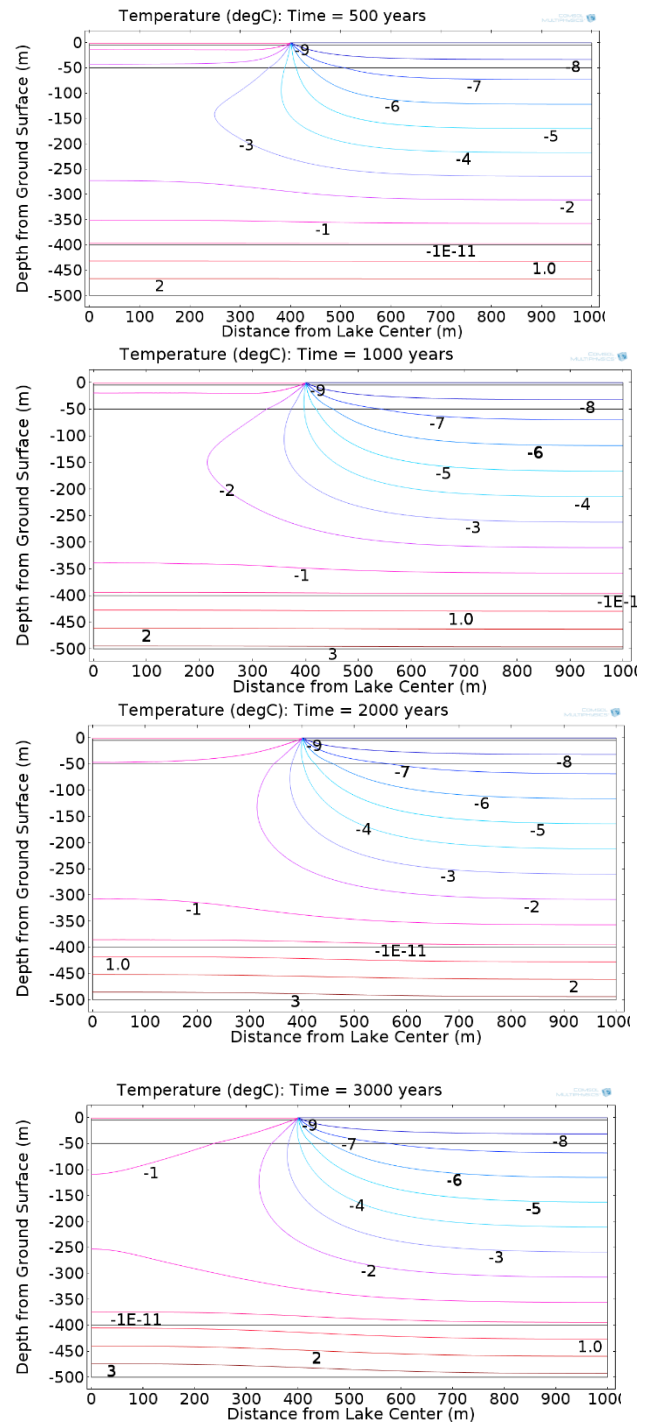


Figure 5. Simulation Results of the Verification Model run at Steady-State in COMSOL



Case C4 Results
(Ling and Zhang, 2003)



Verification Results in
COMSOL

Figure 4. Comparison of Case C4 Results of Ling and Zhang (2003) and Model Verification in COMSOL

5. Discussion

Regarding the verification results provided in Figure 4, the results from COMSOL are very close to those published by Ling and Zhang (2003). At 500 years each isotherm is equally aligned with those by Ling and Zhang (2003). The exception to this is the top of the -2°C at a depth of -55 m, compared to -120 m illustrated by Ling and Zhang (2003). This is an interesting result as there is no difference in the computations used to calculate the -2°C isotherm and all other temperatures less than -1°C .

At 1000 years and 2000 years the simulation results from both Ling and Zhang (2003) and those performed in COMSOL are identical. At 3000 years again there is a single difference. This is evident from the -1°C isotherm has overshoot that of Ling and Zhang (2003). The top of the isotherm is at a depth of -130 m while the bottom is at -230 m compared to Ling and Zhang (2003) results at -90 m and -290 m.

The most central explanation for the slight variations between the simulation results of Ling and Zhang (2003) and those performed in the verification study is the model itself. Ling and Zhang (2003) developed a model to simulate highway thermal stability analysis in permafrost regions, and modified this model for the purpose of their study with regards to talik development under shallow thaw lakes (Ling and Zhang 2003). The verification study utilized the sophistication of COMSOL software which includes various internal solvers and smoothing functions used to obtain convergence and calculate an approximation to the solution using FEM. The difference in model sophistication is very likely the reason for slight differences in the results. Other explanations include the mesh size, and step size of the simulation time.

With regards to the steady-state solution in Figure 5, under the assumption of a constant lake bottom temperature of 0°C and an annual mean permafrost surface temperature of -9°C , the extent of the thaw bulb increases significantly past that at 3000 years even influencing the soil underneath the ground surface near the lake bottom.

6. Conclusions

The graphical comparison of the simulation results show that they are in agreement with those published by Ling and Zhang (2003). In light of the obtained results, COMSOL can be used to adequately model the time-dependent conductive heat transfer with phase change and assess the thaw effects due to a shallow thaw lake over continuous permafrost. The verification of this study provides evidence that the COMSOL code can be applied to more complex multiphysics problems. This includes the modelling of coupled heat transfer (conduction and convection with phase change) and groundwater flow in order to determine the thaw effects surrounding a uranium in-pit TMF in continuous permafrost.

7. References

1. Ling, F., and Zhang, T. 2003. Numerical simulation of permafrost thermal regime and talik development under shallow thaw lakes on the Alaskan Arctic Coastal Plain. *Journal of Geophysical Research*, 108(D16), 4511
2. Andersland, O. B. and Ladanyi, B. (2004). *Frozen Ground Engineering* (Second ed.). Hoboken, New Jersey: John Wiley and Sons, Inc.
3. Burn, C. R. (2002). Tundra lakes and permafrost, Richards Island, western Arctic coast, Canada. *Canadian Journal of Earth Sciences*, 39, 1281-1298.
4. Lawrence, D. M. Slater, A. G. Tomas, R. A. Holland, M. M. and Deser, C. (2008). Accelerated Arctic land warming and permafrost degradation during rapid sea ice loss. *Geophysical Research Letters*, 35(L11509), 1-6.
5. Johnston, G. H. and Brown, R. (1964). Some observations on permafrost distribution at a lake in Mackenzie delta, N.W.T. Canada Arctic. *ARCTIC: Journal of the Arctic Institute of North America*, 17(3), 162-175.
6. Biggar, K. W. (2004). Contaminant Behaviour and Impact in Permafrost Soils - A Review Processes and Potential Impacts, submitted to Brian Heppelle, Environment Canada, Northern Division.

7. Dyke, L. D. (2001). Contaminant migration through the permafrost active layer, Mackenzie Delta area, Northwest Territories, Canada. *Polar Record*, 37(202), 215-228.
8. Tokarev, I. Zubkov, A. A. Rumynin, V. G. Polyakov, V. A. Kuznetsov, V. Y. and Maksimov, F. E. (2006). Origin of high $^{234}\text{U}/^{238}\text{U}$ ratio in post-permafrost aquifers. In B. J. Merkel, and A. Hasche-Berger, *Uranium in the Environment: Mining Impact and Consequences* (pp. 847-856). Berlin/Heidelberg, DEU: Springer.
9. Surbeck, H. Kies, A. and Aviolat, P. (2006). Possible influence of permafrost melting on $^{234}\text{U}/^{238}\text{U}$ activity ratios in Alpine groundwater. 4th Swiss Geoscience Meeting. Bern.
10. Farouki, O. T. (1981). *Thermal Properties of Soils*. U.S. Army Cold Regions Research and Engineering Laboratory Monograph 81-1.
11. Kersten, M. S. (1949). *Laboratory Research for the Determination of the Thermal Properties of Soils*. ACFEL Technical Report 23, AD71256 (Also: *Thermal properties of soils*. University of Minnesota Engineering Experiment Station Bulletin No. 28).
12. Lunardini, V. J. (1981). *Heat Transfer in Cold Climates*. New York: Van Nostrand Reinhold.
13. Anderson, D. M. and Tice, A. R. (1972). Predicting unfrozen water contents in frozen soils from surface area measurements. In n. A. Sciences, *Frost Action in Soils* (pp. 12-18). Washington, D.C.
14. Tice, A. R. Anderson, D. M. and Banin, A. (1976). *The Prediction of Unfrozen Water Contents in Frozen Soils from Liquid Limit Determinations*. U.S. Army Cold Regions Research and Engineering Laboratory Report CRREL 76-8.
15. Ling, F. Yan, D. and Qian, Z. (2000b). Numerical Investigation of thermal regime of roadbed under different type of driving surfaces in Huashixia Valley, China. *Journal Glaciology and Geocryology*, 22 Supl, 118-121.
16. Ling, F. Zeng, Z. and Zhang, L. (2000a). The effect of construction of revetment in the side of embankment. In J. F. Thimus, *Ground Freezing 2000* (pp. 43-46). Balkema.